EASR

Engineering and Applied Science Research

https://www.tci-thaijo.org/index.php/easr/index

Published by the Faculty of Engineering, Khon Kaen University, Thailand

Damage evaluation of fiber-reinforced concrete exposed to elevated temperatures by nondestructive tests

Prae Suwanvitaya[1)], Piya Chotickai*[1)] and Otsuki Nobuaki[2)]

[1)]Department of Civil Engineering, Faculty of Engineering, Kasetsart University, Bangkok 10900, Thailand
[2)]Department of International Development of Engineering, Tokyo Institute of Technology, Tokyo, Japan

Received 28 September 2018
Revised 14 October 2018
Accepted 16 October 2018

Abstract

The paper presents a methodology for damage evaluation of fiber-reinforced concrete (FRC) exposed to elevated temperatures of 400 °C to 800 °C. The residual compressive strength fraction of cylindrical FRC specimens with a water–cement ratio of 0.47 and total fiber volume fraction of 1.2% was evaluated for mixtures with various proportions of steel and polypropylene fibers. The residual compressive strength fraction increased with the increase in the proportion of steel fiber at 400 °C. The residual strength fractions of mixtures with various fiber proportions changed less with increased exposure temperature. The effectiveness of visual inspection and ultrasonic nondestructive tests in assessing the effects of temperature exposure and the residual compressive strength fraction was evaluated. The experimental results indicate a potential application of the nondestructive tests on damage assessment of FRC with various mixture proportions. An equation for estimating the residual compressive strength fraction based on ultrasonic pulse velocity was developed.

Keywords: Fiber reinforced concrete, High temperature, Residual strength, Ultrasonic pulse velocity, Visual inspection

1. Introduction

Concrete is generally recognized as good fire-resistant construction material. However, at elevated temperatures it is subjected to chemical and physical degradation [1-2]. This breakdown results in spalling, cracking, and loss of strength and stiffness of concrete members. At temperatures of 100 °C to 250 °C, water contained in micropores evaporates and ettringite in hydrated cement dehydrates [3]. The dehydration of calcium hydroxide occurs at temperatures between 450 °C and 550 °C. Dehydration of calcium-silicate hydrates occurs at about 700 °C. These dehydrations result in decomposition and weight loss of concrete. Thermal dilation and vaporization of unbound and bound water causes concrete-cover spalling. Damage severity increases with heating rate and concrete strength.

Short fibers are widely used in the reinforcement of concrete to improve its mechanical properties and durability. The short discrete fibers added during concrete mixing are uniformly distributed and randomly oriented in fiber-reinforced concrete (FRC). Due to the crack bridging effect provided by fibers [4], post-cracking strength and toughness of concrete can be significantly increased. The improvements in strength and fracture toughness of steel fiber-reinforced concrete (SFRC) are extensively reported in the literature [5-6]. Polypropylene (PP) fiber has been reported to reduce shrinkage and increase durability of concrete [7]. A combination of steel and PP fibers is used in hybrid FRC to obtain optimal performance of concrete material [8]. For concrete exposed to elevated temperatures, previous studies [9-10] have shown that use of polypropylene (PP) and steel fibers reduces cracking and spalling of FRC. The PP fiber melts and vaporizes at approximately 170 °C and 340 °C, respectively [11]. An increase in the permeability of concrete reduces the built-up pore pressure and reduces the probability of spalling. A negative effect of PP fiber on the compressive strength of concrete has been reported [12]. Steel fiber reduces pore pressure in concrete, but to a lesser extent. The reduction in pore pressure in steel fiber-reinforced concrete is associated with discrete bubbles developed during mixing [13]. In a previous study [14], steel fiber was shown to be useful in minimizing damage and enhancing the residual compressive strength of heated concrete. Steel fiber also improves the tensile strength, ductility, and toughness of concrete at ambient temperatures.

Nondestructive techniques for post-fire damage assessment are essential for estimating the residual strength of concrete members. Previous studies [15-16] show a strong relationship between the residual strength fraction and the residual ultrasonic pulse velocity (UPV) fraction of conventional concrete exposed to elevated temperatures. The water-to-cement ratio is reported to insignificantly affect the residual strength fraction and residual UPV fraction for mixtures exposed to elevated temperatures. The UPV has been shown to be a promising damage indicator of

*Corresponding author. Tel.: +6689 166 8897
Email address: fengpyc@ku.ac.th
doi: 10.14456/easr.2019.5

Table 1 Property of Fibers

Property	Hooked-end Steel Fiber (SF)	PP Fiber
Length (mm)	35	12
Diameter (mm)	0.55	32×10^{-3}
Specific Gravity	7.8	0.91
Tensile Strength (MPa)	1,350	400
Modulus of Elasticity (MPa)	210,000	3500

Table 2 Specimen Details

Specimen	Fiber Volume Fraction (%)		Number of Specimens
	Hooked-end Steel Fiber (SF)	PP Fiber	
M1	1.2	0	12
M2	0.9	0.3	12
M3	0.6	0.6	12
M4	0.3	0.9	12
M5	0	1.2	12
M6	0	0	12

FRC exposed to temperatures of up to 400 °C [17].

The two primary objectives of this study are (i) to evaluate the effects of elevated temperatures on the residual compressive strength fraction of FRC with various mixture proportions of hooked-end steel and PP fibers, and (ii) to evaluate the effectiveness of visual inspection and ultrasonic nondestructive tests on damage assessment. Mixtures with relatively high strength were exposed to elevated temperatures of up to 800 °C. The mechanical properties of the specimens after such exposure were evaluated and related to the results obtained from nondestructive testing.

2. Materials and methods

The experimental program consisted of compressive strength and nondestructive tests of cylindrical FRC specimens. Nondestructive tests were conducted on the specimens before and after exposure to elevated temperatures.

2.1 Specimen preparation

Cylindrical specimens that were 100 mm in diameter and 200 mm in height were prepared from Portland cement Type 1, river sand, and crushed stone with a maximum nominal size of 19 mm. A water-to-cement ratio of 0.47 was used in all specimens, with various proportions of hooked-end steel and PP fibers. Superplasticizer was used to keep the slump at 12 mm. The steel fiber had a nominal length of 35 mm and a diameter of 0.55 mm, whereas the PP fiber had a nominal length of 12 mm and a diameter of 32×10^{-3} mm, as presented in Table 1.

The specimens were prepared using various mixture proportions of steel and PP fibers, as presented in Table 2. Specimens M1 and M5 had a 1.2% volume of steel and PP fibers, respectively. Specimens M2 to M4 were hybrid fiber-reinforced concrete (HFRC) with a mixture of steel and PP fibers. Specimen M6 was a reference concrete sample with no fibers. During the concrete mixing, the fibers were gradually added to the mixing machine to achieve uniform fiber distribution in the mixtures. After casting, the specimens were wet cured for 28 days and subsequently dried in ambient air before exposure to elevated temperatures of 400 °C, 600 °C, and 800 °C. Twelve specimens were prepared from each concrete mixture. Three of the specimens were kept at room temperature (25 °C), while the other specimens were subjected to the elevated temperatures in an electrically heated furnace. During heating, the temperature was increased at a rate of 5 °C per hour until the target temperature was reached, and maintained constant at the target temperature for 1 h. The specimens were subsequently cooled to room temperature in the furnace for 24 h before subjected to nondestructive and compressive strength tests.

2.2 Compressive strength and nondestructive tests

The specimens were subjected to a compressive strength test using a universal testing machine. Axial force was applied at a displacement-controlled rate of 0.25 mm/min. The applied load and longitudinal deformation were recorded during the test.

Two nondestructive tests were employed in the study, visual inspection and an ultrasonic testing method. The dimensions, crack width, and images of all sides of the specimens were recorded during the visual inspection. A Vernier caliper with a precision of 0.01 mm was used to measure the specimen diameters at three locations and heights at four locations, as presented in Figure 1a. The measurement locations were marked using heat-resistant marker pens to obtain the same reading locations both before and after the exposure. The maximum crack widths in the specimens after being cooled in ambient air for 24 h were measured using a crack gauge with a sensitivity of 0.5 mm.

An ultrasonic testing method was conducted using a Pundit Lab ultrasonic measurement instrument with a pair of 54-kHz nominal frequency transducers. The UPV was computed from the travel time of the ultrasonic wave to propagate through concrete between the transmitting and receiving transducers, and the measured distance between the transducers [18]. Direct transmission mode, in which the transducers were located directly opposite each other, was along the longitudinal axis of the cylinder specimens, as presented in Figure 1b. Measurements were made three times on each specimen, both before and after the exposure, to obtain reliable results.

Table 3 Experimental Results of Testing Concrete Cylinder Specimens

Mix	Fiber Volume Fraction (SF:PP)	Temperature (°C)	Compressive Strength		UPV	
			Ave. (MPa)	Std. (MPa)	Ave. (m/s)	COV (%)
M1	1.2:0.0	25	38.0	4.5	4755	1.4
		400	32.9	0.3	3722	3.4
		600	20.7	1.5	2032	3.2
		800	10.0	1.8	1470	15.0
M2	0.9:0.3	25	43.0	4.0	4391	2.6
		400	34.4	4.5	3727	1.3
		600	18.2	5.3	1819	12.0
		800	12.0	0.3	1196	3.0
M3	0.6:0.6	25	38.0	4.2	4445	2.1
		400	26.4	3.4	3377	3.5
		600	16.5	2.1	1330	9.6
		800	9.4	0.8	924	22.6
M4	0.3:0.9	25	30.3	8.0	4269	0.2
		400	20.9	3.2	3224	4.1
		600	14.2	2.1	1355	7.8
		800	7.5	0.3	597	2.1
M5	0.0:1.2	25	30.3	6.5	4405	4.4
		400	17.4	1.5	3092	1.1
		600	13.2	1.7	1105	17.0
		800	6.8	0.3	622	12.3
M6	0.0:0.0	25	40.6	9.4	4751	2.8
		400	26.1	6.3	3726	0.6
		600	15.5	3.1	1399	3.6
		800	9.1	0.7	846	19.9

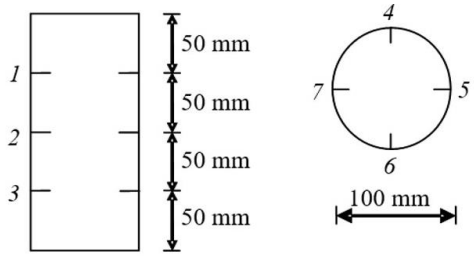

a) Locations for transverse (1, 2, 3) and longitudinal dimension measurement

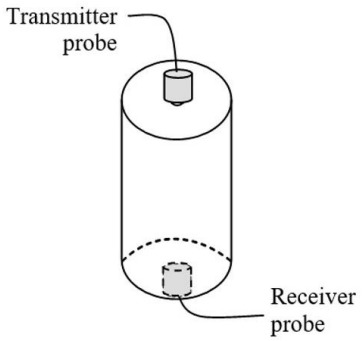

b) Ultrasonic test (4, 5, 6, 7) dimension measurement

Figure 1 Measurement locations for nondestructive tests

3. Results

The results obtained from the compressive strength tests are presented in Table 3. The average compressive strength of specimen M6 before heat exposure was 40.6 MPa. No significant increase in the compressive strength was observed in the mixture with steel fibers (specimen M1). Meanwhile, a decrease in the compressive strength was obtained from the specimens with a high proportion of PP fibers. Specimen M5 with the highest volume fraction of PP fiber (1.2%) showed an average compressive strength of 30.3 MPa, corresponding to a 25.4% reduction in this value. This could be attributed to the formation of multifilament structures and the increase in the void volume of the mixtures with PP fibers [9].

Typical stress–strain curves of the concrete mixtures exposed to elevated temperatures are presented in Figure 2. Axial strains were determined from the total shortening of the concrete specimens monitored while using the universal testing machine. The stress–strain curves in the figure exhibit a linear relationship at low stress levels. The initial slope and descending slope after the peak were influenced by the fiber mixture proportions and temperatures. With an increase in the exposed temperatures, the descending paths were less steep. At 400 °C, a significant reduction in the initial slope was observed in specimen M5 with PP fibers. This was caused by voids from fiber vaporization at 340 °C and micro-cracks that developed in the specimens. A significant reduction in the initial slope was observed in specimen M1, containing steel fibers and exposed to heat at 600 °C. The effect of the fibers on the specimens' stiffness was insignificant at 800 °C owing to the degradation of concrete at this temperature. With increased exposure temperature, the strain at the peak stress increased corresponding to a lower value of the initial slope.

The effect of temperature exposure on the average compressive strength of various mixtures is presented in Figure 3a. The average compressive strengths decreased linearly with increased e exposure temperature from 400 °C to 800 °C. The variation in the average compressive strength of the specimens with various mixtures also decreased with the increased exposure temperature.

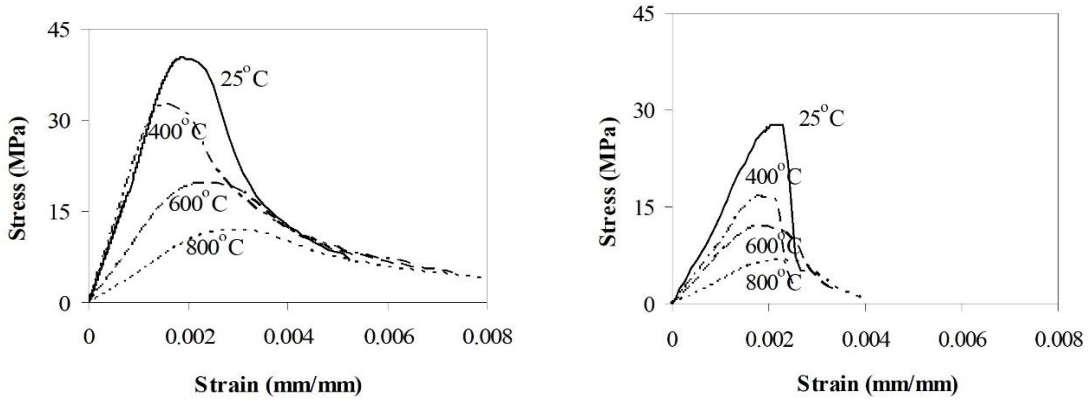

a) M1 (SF:PP = 1.2:0.0) b) M5 (SF:PP = 0.0:1.2)

Figure 2 Stress–strain curves of specimens exposed to elevated temperatures

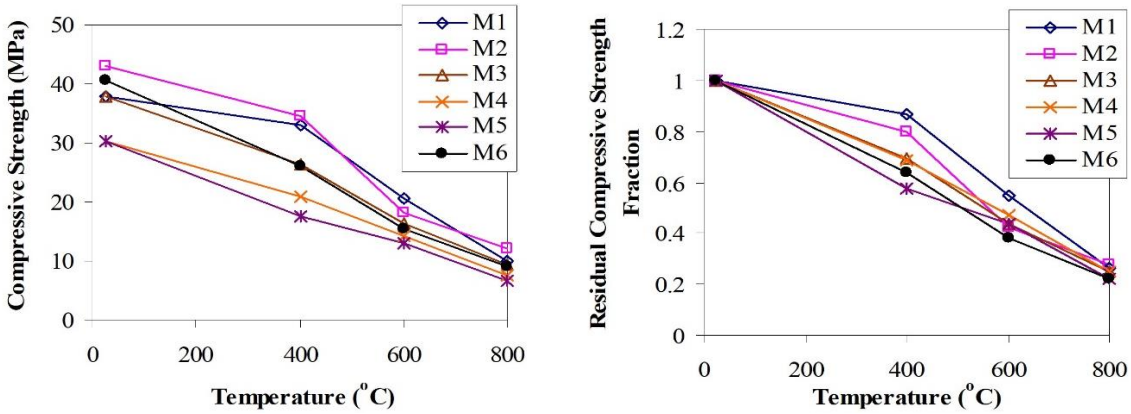

a) Compressive strength b) Residual compressive strength fraction

Figure 3 Effects of temperature on compressive strength and compressive strength fraction

The relationship between the residual compressive strength fraction and temperature is presented in Figure 3b. The residual compressive strength fraction is the ratio between the average compressive strength after heat exposure and that of the unheated specimen. At 400 °C, specimen M1 exhibited the highest compressive strength fraction of 0.87. With a decreased level of steel fiber, the fractions decreased to the values of 0.80 and 0.69 in specimens M2 and M3, respectively. This indicates that the steel fiber retarded the reduction in compressive strength at 400 °C. The compressive strength fraction, 0.58, in specimen M5 was slightly lower than the value obtained from specimen M6, 0.64. No compressive strength enhancement by the PP fiber on the specimens subjected to the heat exposure was observed. The variation in the residual compressive strength fraction decreased with increased exposure temperature. At 800 °C, the residual compressive strength fractions of the various mixtures were between 0.22 and 0.26.

4. Discussion

4.1 Visual inspection

The effect of exposure temperature on the percentage change in the diameter and volume of the specimens is presented in Figure 4. At 400 °C, specimen M6 showed a reduction in the diameter and volume owing to the loss of bound and unbound water. The expansion at elevated temperatures of 600 °C and 800 °C remained after cooling, thus resulting in residual expansion at these temperatures. Specimen M1 showed an increase in the diameter and volume at 400 °C. This indicated that the effect of steel fiber in preventing dimension recovery was more dominant than the contraction due to the loss of water in the specimen. At 800 °C, specimen M1 showed a lower percentage of dimensional change than did specimen M6. The PP fiber melted at a temperature greater than 160 °C, providing voids for concrete expansion at elevated temperatures. Consequently, specimen M5, with the highest percentage of PP fiber, tended to show the least percentage of dimensional change at almost all elevated temperatures.

The average maximum crack widths of the specimens are presented in Figure 5. No cracks were observed in the specimens exposed to 400 °C. At 600 °C, the average maximum crack widths of the specimens with various fiber proportions were in the same range, between 0.1 mm and 0.15 mm. The maximum crack width of the mixture with no fibers (M6) was in the same range as the other specimens. This is attributable to the low heating rate used in the study. At 800 °C, a significant increase in the average maximum crack width, 0.28 mm, was obtained from specimen M5. The M2 to M5 specimens with PP fibers exhibited a greater maximum crack width than specimen M6. This indicates an adverse effect of PP fibers on the crack width at the elevated temperatures.

A comparison of the color of specimen M1 after it was exposed to various temperatures is presented in Figure 6. The grey color of the control specimen changed to a reddish-brown after exposure to 400 °C and 600 °C, and white grey at 800 °C. The reddish-brown color was associated with the presence of iron compounds in the aggregates [19]. Siliceous aggregates have a wide variety of

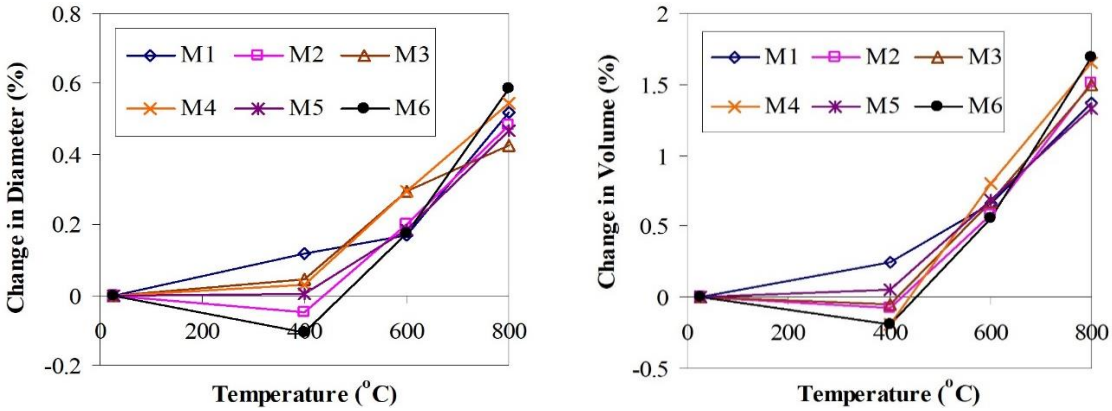

a) Change in diameter b) Change in volume

Figure 4 Effect of temperature on change in specimen dimensions

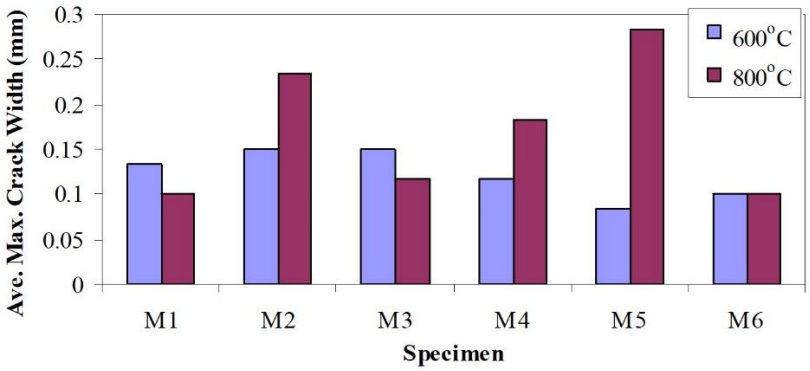

Figure 5 Effect of temperature on average maximum crack width

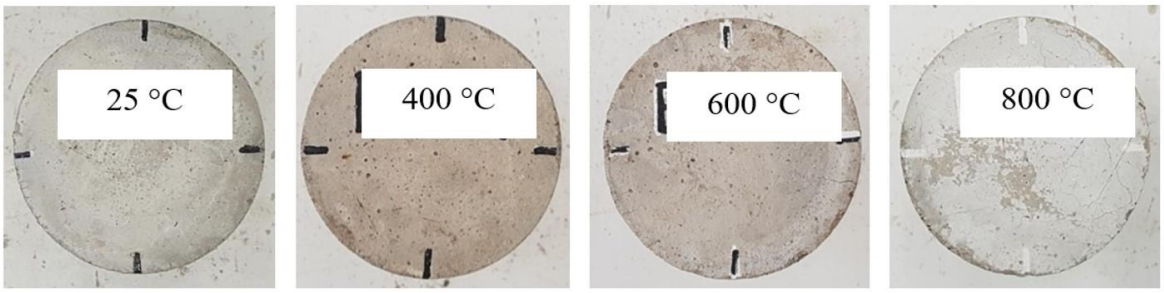

Figure 6 Effect of temperature on the color of specimen M1

colors at ambient temperature. They generally start to turn pink around 250-300 °C due to the oxidation of iron ions, while calcareous aggregates are black at ambient temperature start to turn white due to decarbonation around 700 °C [20]. No significant difference in discoloration of specimens with various mixtures of fibers was observed after exposure to heat.

4.2 Ultrasonic testing

The results of ultrasonic testing are presented in Table 3 and Figure 7. The average UPV of the unheated specimen M6 was 4750 m/s. This value was relatively close to the value of 4775 m/s of specimen M1. No significant increase in the UPV of unheated specimens with 1.2% volume of steel fiber was obtained. The wave speed, however, decreased slightly to a value of 4405 m/s in specimen M5, corresponding to the lower compressive strength of the specimen. The UPVs of the specimens with various mixtures decreased to the values between 3092 m/s and 3726 m/s at 400 °C, and 622 m/s to 1470 m/s at 800 °C.

The effect of temperature on the residual UPV fraction is presented in Figure 7b. The residual UPV fraction is the ratio of the UPV after the exposure and that of the unheated specimen. Specimens M1 and M2 showed a relatively similar range of residual UPV fractions, and were greater than those of the other specimens at all elevated temperatures. Meanwhile, specimen M5 exhibited the lowest residual UPV fraction.

The relationship between the residual compressive strength fraction and the residual UPV fraction is presented in Figure 8. The residual compressive strength fraction exhibited a linear relationship, showing a very strong correlation with the residual UPV fraction for various concrete mixtures. This indicates the potential application of the UPV in damage assessment of fiber-reinforced

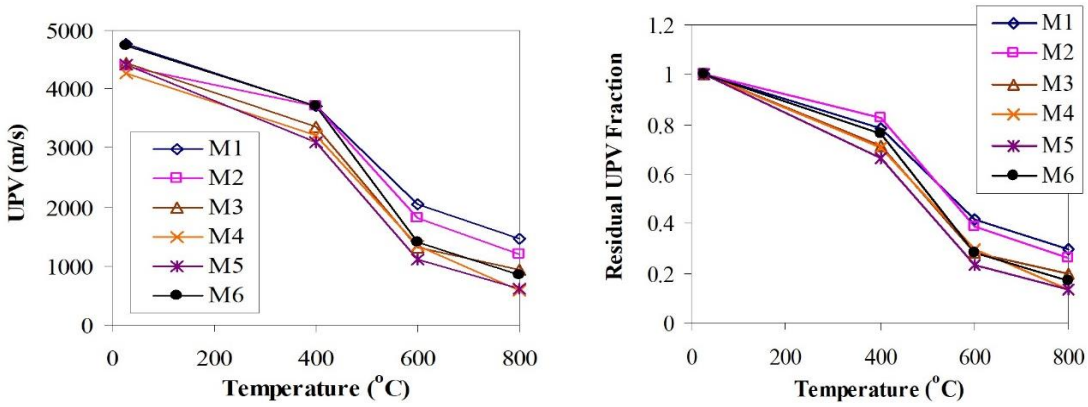

a) UPV b) Residual UPV fraction

Figure 7 Effects of temperature on UPV and UPV fraction

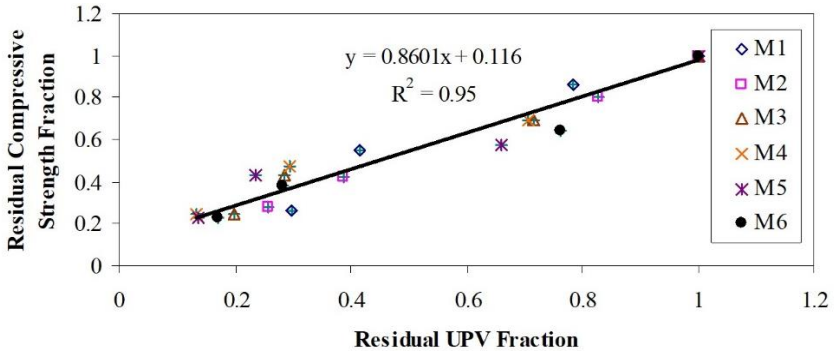

Figure 8 Relationship between residual compressive strength and residual UPV fraction

concrete. For all residual UPV fractions, the maximum difference between the actual and computed strength fractions provided by the equation in the figure is 0.13.

5. Conclusions

Experiments were performed to evaluate the effects of mixture proportions of steel and PP fibers on the compressive strength of the concrete specimens exposed to elevated temperatures between 400 °C and 800 °C. The compressive strengths of the specimens with various fiber proportions were determined both before and after heat exposure. Visual inspection and ultrasonic nondestructive tests were performed for damage and residual strength fraction assessments. Based on the experimental results, the following conclusions were obtained:

1. No significant increase in the compressive strength was obtained in the specimens with 1.2% volume of steel fiber. An increased level of PP fiber, however, reduced the compressive strength of the unheated and heated specimens.

2. Steel fibers effectively retarded the reduction in the compressive strength of the specimens exposed to elevated temperatures, particularly at 400 °C. The difference in the compressive strengths of the specimens with various fiber proportions decreased with increased exposure temperature.

3. The average maximum crack widths of all concrete mixtures were in the same range at 600 °C. However, at 800 °C, the concrete mixture with a high fraction of PP fiber exhibited the highest average crack width.

4. No significant effect of the fiber proportion and type on the specimen discoloration was observed. This indicated possible application of a discoloration parameter in estimating the exposure temperature of mixtures with various fiber types and proportions.

5. A linear relationship with strong correlation between the residual compressive strength fraction and the residual UPV fraction was obtained. Potentially, the UPV could be used for estimating the residual compressive strength fraction of FRC.

6. Acknowledgements

The support and assistance of Miss Sukanya Teerapong and Mr. Watthanai Assapattarapun are gratefully acknowledged.

7. References

[1] Jameran A, Ibrahim IS, Yazan SHS, Rahim, SNA. Mechanical properties of steel-polypropylene fibre reinforced concrete under elevated temperature. Procedia Engineering. 2015;125:818-24.

[2] Felicetti R, Monte FL, Pimienta P. A new test method to study the influence of pore pressure on fracture behaviour of concrete during heating. Cement Concr Res. 2017;94:13-23.

[3] Balázs GL, Lublóy É. Post-heating strength of fiber-reinforced concretes. Fire Saf J. 2012;49:100-6.

[4] Aly T, Sanjayan JG, Collins F. Effect of polypropylene fibers on shrinkage and cracking of concretes. Mater Struct. 2008;41:1741-53.

[5] Olivito RS, Zuccarello FA. An experimental study on the tensile strength of steel fiber reinforced concrete. Compos B Eng. 2010;41(3):246-55.

[6] Sappakittipakorn M, Sukontasukkul P, Higashiyama H, Chindaprasirt P. Properties of hooked end steel fiber reinforced acrylic modified concrete. Construct Build Mater. 2018;186:1247-55.
[7] Cifuentes H, García F, Maeso O, Medina F. Influence of the properties of polypropylene fibres on the fracture behaviour of low-, normal- and high-strength FRC. Construct Build Mater. 2013;45:130-7.
[8] Huang L, Xu L, Chi Y, Xu H. Experimental investigation on the seismic performance of steel-polypropylene hybrid fiber reinforced concrete columns. Construct Build Mater. 2015;87:16-27.
[9] Poon CS, Shui ZH, Lam L. Compressive behavior of fiber reinforced high-performance concrete subjected to elevated temperatures. Cement Concr Res. 2004;34(12):2215-22.
[10] Bangi MR, Horiguchi T. Effect of fibre type and geometry on maximum pore pressures in fibre-reinforced high strength concrete at elevated temperatures. Cement Concr Res. 2012;42(2):459-66.
[11] Zeiml M, Leithner D, Lackner R, Mang HA. How do polypropylene fibers improve the spalling behavior of in-situ concrete?. Cement Concr Res. 2006;36(5): 929-42.
[12] Chan YN, Luo X, Sun W. Compressive strength and pore structure of high-performance concrete after exposure to high temperature up to 800ºC. Cement Concr Res. 2000;30(2):247-51.
[13] Bangi MR, Horiguchi T. Pore pressure development in hybrid fibre-reinforced high strength concrete at elevated temperatures. Cement Concr Res. 2011;41(11):1150-6.
[14] Lau A, Anson M. Effect of high temperatures on high performance steel fibre reinforced concrete. Cement Concr Res. 2006;36(9):1698-707.
[15] Yan H, Lin Y, Hsiao C, Liu JY. Evaluating residual compressive strength of concrete at elevated temperatures using ultrasonic pulse velocity. Fire Saf J. 2009;44(1):121-30.
[16] Lin Y, Hsiao C, Yang H, Lin YF. The effect of post-fire-curing on strength-velocity relationship for nondestructive assessment of fire-damaged concrete strength. Fire Saf J. 2011;46(4):178-85.
[17] Suhaendi SL, Horiguchi T. Effect of short fibers on residual permeability and mechanical properties of hybrid fibre reinforced high strength concrete after heat exposition. Cement Concr Res. 2006;36(9): 1672-8.
[18] American Society for Testing and Materials. ASTM C597-16: 2016. Standard test method for pulse velocity through concrete. PA: ASTM; 2016.
[19] Georgali B, Tsakiridis PE. Microstructure of fire-damaged concrete. a case study. Cement Concr Compos. 2005;27(2):255-9.
[20] Annerel E, Taerwe L. Methods to quantity the colour development of concrete exposed to fire. Construct Build Mater. 2011;25:3989-97.